https://doi.org/10.5194/nhess-2020-47
Preprint. Discussion started: 24 February 2020

Natural Hazards and Earth System Sciences
Discussions

Wide sensitive area of small foreshocks

Chieh-Hung Chen[1,2*], Yang-Yi Sun[1], Strong Wen[3], Peng Han[4], Li-Ching Lin[5], Huai-Zhong Yu[6], XueMin Zhang[7], Yongxin Gao[8], Chi-Chia Tang[1,2], Cheng-Horng Lin[9], Jann-Yenq Liu[10,11,12]

1. Institute of Geophysics and Geomatics, China University of Geosciences, Wuhan, China
2. State Key Laboratory of Geological Processes and Mineral Resources, Institute of Geophysics and Geomatics, China University of Geosciences, Wuhan, China
3. Department of Earth and Environmental Sciences, National Chung Cheng University, Chia-Yi, Taiwan
4. Department of Earth and Space Sciences, Southern University of Science and Technology, Shenzhen, China
5. Science and Technology Policy Research and Information Center Taiwan, Taiwan
6. China Earthquake Networks Center, Beijing, China
7. Institute of Earthquake Forecasting, China Earthquake Administration, Beijing, China
8. School of Civil Engineering, Hefei University of Technology, Hefei, China
9. Institute of Earth Sciences, Academia Sinica, Taipei, Taiwan
10. Graduate Institute of Space Science, National Central University, Taoyuan, Taiwan
11. Center for Astronautical Physics and Engineering, National Central University, Taoyuan, Taiwan
12. Center for Space and Remote Sensing Research, National Central University, Taoyuan, Taiwan

* **Corresponding Author:**
Chieh-Hung Chen, E-mail: nononochchen@gmail.com
Institute of Geophysics and Geomatics,

https://doi.org/10.5194/nhess-2020-47
Preprint. Discussion started: 24 February 2020

Natural Hazards and Earth System Sciences Discussions

China University of Geosciences, Wuhan, Hubei, 430074, China

Abstract

Scientists demystify stress changes within tens of days before a mainshock and often utilize its foreshock as an indicator. Typically, foreshocks are detected near fault zones, which may be due to the distribution of seismometers. This study investigates changes in seismicity far from mainshocks by examining tens of thousands of M >= 2 quakes that were monitored by dense seismic arrays for more than 10 years in Taiwan and Japan. The quakes occurred within epicentral distances ranging from 0 km to 400 km during a period of 60 days before and after the mainshocks that are utilized to exhibit common behaviors of seismicity in the spatiotemporal domain. The superimposition results show that wide areas exhibit increased seismicity associated with mainshocks being more than 50 times to areas of the fault rupture. The seismicity increase initially concentrates in the fault zones, and gradually expands outward to over 50 km away from the epicenters approximately 40 days before the mainshocks. The seismicity increases more rapidly around the fault zones approximately 20 days before the mainshocks. The stressed crust triggers resonance at frequencies varying from ~3×10^{-4} Hz to ~10^{-3} Hz (i.e., variable frequency) along with earthquake-related stress that migrates from exterior areas to approach the fault zones. The variable frequency is determined by the observation of continuous seismic waveforms through the superimposition processes and is further supported by the resonant frequency model. These results suggest that the variable frequency of ground vibrations is a function of areas with increased seismicity leading to earthquakes.

Keywords: foreshocks; resonance frequency; earthquake-related stressed area

1. Introduction

Numerous studies (Reasenberg, 1999; Scholz, 2002; Vidale et al., 2001; Ellsworth and Beroza, 1995) reported that foreshocks occur near a fault zone and migrate toward the hypocenter of a mainshock before its occurrence. The spatiotemporal evolution of foreshocks is generally considered to be an essential indicator that reveals variations in earthquake-related stress a couple of days before mainshocks. After detecting these variations, scientists installed multiple instruments along both sides of the fault to monitor over short distances to monitor the activity of the fault. However, these instruments typically detect small vibrations near the fault zone. Stress accumulates in a local region near a hypocenter triggering earthquake occurrence that is concluded from the sparse distribution of seismometers.

It is a big challenge to monitor stress changes in a wide area beneath the ground. A simple way to imagine this is if we place a stick on a table then hold and try to break the stick. The stress we making on the stick can apply to either a limited local region or to both ends of it. Migrations and propagations of loading force can be detected according to the changes of strain and the occurrence of microcracks. This common sense suggests that the spatiotemporal evolution of earthquake-related stress appearing a couple of days before mainshocks can be recognized if we can trace the occurrence of relatively-small quakes in a wide area (Kawamura et al., 2014; Wen and Chen, 2017). Here we take advantage of earthquake catalogs obtained by dense seismic arrays in Taiwan and Japan to expose foreshocks distributing over a wide area instead of a local region.

2. Methodology

The ability to detect relatively-small quakes depends on the spatial density and capability of seismometers. Taiwan and Japan are both the most famous high-seismicity areas in the world. Dense seismometers evenly distributed throughout the whole area are beneficial for monitoring the occurrence of earthquakes both near to and far away from fault zones (Chen, 2014). Earthquake catalogs retrieved of Taiwan and Japan were obtained from the Central Weather Bureau, and the Japan Meteorological Agency (JMA), respectively. The ZMAP software package for MATLAB (Weimer,

https://doi.org/10.5194/nhess-2020-47
Preprint. Discussion started: 24 February 2020

Natural Hazards and Earth System Sciences
Open Access
Discussions

2001) was utilized to remove and/or omit influence from duplicate events, such as aftershocks. We classify clusters by using the standard input parameters (proposed in Reasenberg, 1985 and Uhrhammer, 1986) for declustering algorithm. The minimum and maximum values of the look-ahead time for building clusters are 1 and 10, respectively. The probability of detecting the next clustered event used to compute the look-ahead time is 0.95. The effective minimum magnitude cut-off for catalog is given by 1.5 and the xk factor for the increase of the minimum cut-off magnitude during clusters is given by 0.5. The 10 of crack radii surrounding each earthquake within new events considered to be part of the cluster (Stiphout, 2012). Earthquakes with depth > 30 km were eliminated from the declustered catalogs for understanding changes of seismicity before mainshocks mainly in the crust.

Based on the occurrence of the cracks that can be the clues of force loading on a material before its break, all the earthquakes with magnitude >= 2, which are retrieved from the declustered earthquake catalogs, are considered to be the crack events dominated by the force loading on the curst. Note that the minimum magnitudes of completeness Mc is 2.0 and 0.0 in Taiwan and Japan, respectively (also see Figs. S1–S4). This represents the ability of its seismic monitoring network to detect crack events. We construct a spatiotemporal distribution of the crack events for each break quake. The spatiotemporal distribution from 0 km to 400 km away from the epicenter of the break quake during a period of 60 days before and after the break occurrence is constructed to illustrate the relationship between the crack events and the break quake in the spatial and temporal domain. Note that the spatial and temporal resolutions of the grids of the spatiotemporal distribution are 10 km and 1 day, respectively. We count the crack events in each spatiotemporal grid according to distance away from the epicenter and the differences in time before and after the occurrence of the break quake.

The superimposition process, a statistical tool utilized in data analysis, is capable of either detecting periodicities within a time sequence or revealing a correlation between more than two data sequences (Chen, 2014), which is known as the superposed epoch analysis (Adams et al., 2003; Hocke, 2008). The spatiotemporal distributions

https://doi.org/10.5194/nhess-2020-47
Preprint. Discussion started: 24 February 2020

of all the break quakes are superimposed as a total one based on the occurrence time of the break quakes and the distance away from the epicenter of the break quakes. The superimposition is utilized to migrate rare characteristics result from particular break quakes and to enhance the common behaviors of the crack events in the spatiotemporal domain. The total count of the superimposed distribution in each spatiotemporal grid is normalized to seismic density (count/km^2) for comparing to the total number of the break quakes and the related spatial area. Moreover, we compute the average values every distance grid using the seismic densities 60 days before and after the quake. The average values are subtracted from the seismic densities and the obtained differences are divided by the average values in each distance grid to obtain the normalized variation clarifying changes of the seismic density in the spatiotemporal domain.

3. Analytical results

The earthquakes with M >= 2 listed in the declustered catalogs of Taiwan from January 1991 to June 2017 are utilized to construct a spatiotemporal distribution of foreshocks and aftershocks corresponding to the quakes with magnitude >= 3. We superimposed all the M >= 2 events corresponding to the 17993 quakes (M >= 3), which increases the signal-to-noise ratios more than 135 times. The seismic density is more than 1000 times greater in a hot region at a distance of 10 km away from an epicenter (which is generally considered to be the gestation area of foreshocks) than it is in areas located > 200 km from the epicenter (Fig. 1a). Note that the events mainly occur 0–1 day after the quakes that is irrelevant to the smaller distribution 0–1 day before the quakes (also see Figs. 1 and 2). On the other hand, the seismic density with epicentral distance smaller than 50 km (Fig. 1a) suddenly increases before and gradually decreases after the quakes. The irrelevance and the differences of changes rates with epicentral distance smaller than 50 km before and after the quakes clarify that the increase of seismicity before the quakes is not contributed by the seismicity after due to the analytical processes in this study.

The increase of the seismic density within the hot region can be traced for more

https://doi.org/10.5194/nhess-2020-47
Preprint. Discussion started: 24 February 2020

than 50 days before the quakes (Fig. 1a). The increase is stable but become sharp a few days before the quakes. On the other hand, the increase of seismic density is not only always limited within the hot region with time but also extends outward to a distance of over 50 km away from the epicenters about 0–40 days leading up to the occurrence of the quakes (also see Fig. 2a). Note that the expansion of the increase of seismic density becomes mitigation and may no longer be impact a place at distances > 200 km away from the epicenters. The increase of seismicity density before the quakes suggests that the accumulation of the earthquake-related stress in the crust originates from the hot region, and gradually extends to an external place before earthquakes occur. The area of this external place is several times that of a fault rupture zone that is concluded based on the sparse seismic arrays of the past. The seismic density sharply increases a few days before the quakes. The sudden increase suggests that earthquake-related stress accumulates mainly around the hot region, triggering many foreshocks a few days before the M >= 3 earthquakes. Numerous recent studies reported that the seismicity migrates toward the fault rupture zone within tens of kilometers from epicenters a couple of days before earthquakes (Kato et al., 2012, Kato and Obara, 2014; Liu et al., 2019). The superimposition results partially support that the idea of the process of stress migration toward the hot regions of hypocenters a few days before earthquakes.

We then examine the spatiotemporal changes in the seismic density up to the M >= 4 quakes utilizing the same superimposition process (Figs. 1b–c). The expansion of the increase seismic density about 0–40 days leading up to the occurrence of the quakes and the sharply increases of seismic density a few days before the quakes that can be consistently observed using the M >= 4 quakes in Figs. 1b–c. Moreover, we retrieved the Japan's earthquake catalogs between 2001 and 2010 from the Japan Meteorological Agency (JMA) and construct the seismic density distribution using the same analysis process (Figs. 1d–f). Similar results (i.e., the sharply increases of seismic density a few days before the quakes and areas where the increase of the seismicity density is much larger than that of the hot region) can be obtained from the earthquake catalogs

https://doi.org/10.5194/nhess-2020-47
Preprint. Discussion started: 24 February 2020

Natural Hazards and Earth System Sciences
Open Access
Discussions

of Taiwan and Japan.

The normalized variations correspond to seismic density in Fig. 1 are shown in Fig. 2. The radii of the positive normalized variations are approximately 50 km while earthquake magnitude increases from 3 to 6 in Taiwan (Figs. 2a–c). The land area of Taiwan is approximately 250 km by 400 km, which causes underestimation of the seismic density in the spatial domain. In contrast, the positive normalized variations roughly expand along the radii ranging from 50 km to 100 km, while earthquake magnitude increases from 3 to 6 in Japan (Figs. 2d–f). However, variations in the lead time mostly range from 40 days to 20 days, and relationships between the positive normalized variations and the earthquake magnitude can be found neither in Taiwan nor Japan (Fig. 2). If the expansion and the existence of the lead time are true, the next step is to determine the potential mechanism hidden behind this nature.

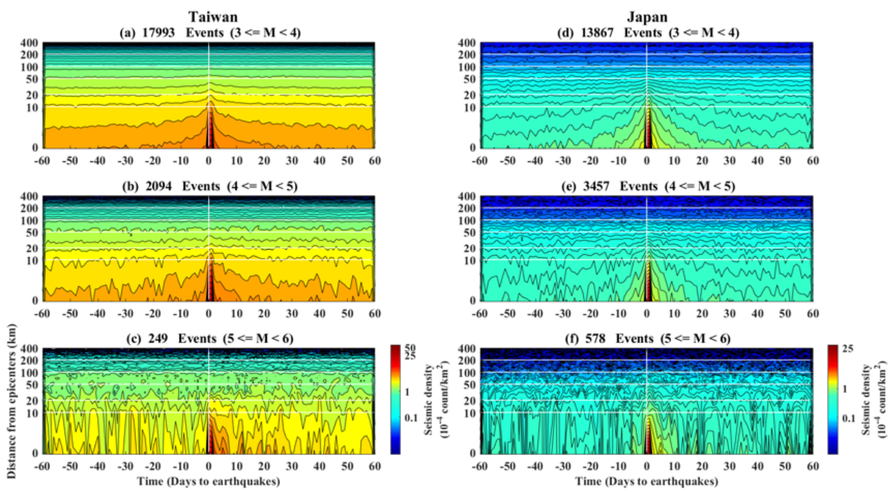

Fig. 1. Spatiotemporal seismic density distributions in Taiwan and Japan. The seismic densities constructed by using the declustered earthquake catalogs of Taiwan and Japan are shown in the left and right panels, respectively. The seismic density reveals changes in seismicity at distances from the epicenters ranging from 0 km to 400

https://doi.org/10.5194/nhess-2020-47
Preprint. Discussion started: 24 February 2020

Natural Hazards and Earth System Sciences
Discussions

km at up to 60 days before and after quakes in a particular magnitude group. We superimposed earthquake numbers by using the differences in time and distance between all the M >= 2 events related to each quake in a particular magnitude group. The superimposed number in each grid is further normalized for a fair comparison by using the total number of quakes and their areas. Notably, the total number of quakes is shown in the title of each diagram.

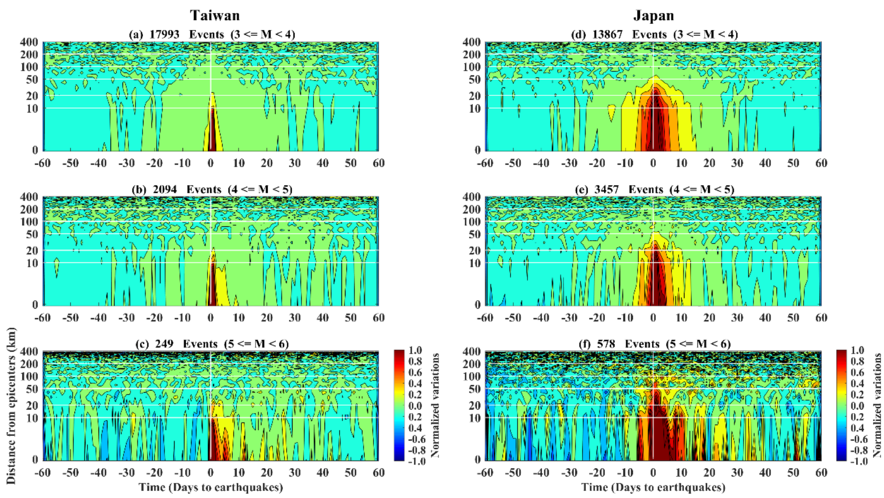

Fig. 2. Changes of spatiotemporal normalized variations in Taiwan and Japan. The normalized variations correspond to the seismic density in Taiwan and Japan (in Fig. 1) are shown in the left and right panels, respectively. The colors reveal changes of the normalized variations at distances from the epicenters ranging from 0 km to 400 km at up to 60 days before and after quakes in a particular magnitude group.

4. Discussions

If an M >= 3 quake can excite seismicity changes over a wide area (i.e., over 50 km by 50 km), any vibration related to stress accumulation before earthquakes can be too small to be identified from raw seismic waveforms. The principal component analysis (PCA) method (Jolliffe, 2002) is utilized to retrieve the possible stress-related vibrations from continuous seismic waveforms recorded at most seismic stations over

https://doi.org/10.5194/nhess-2020-47
Preprint. Discussion started: 24 February 2020

a wide area and to simultaneously mitigate local noise. Seismic waveforms obtained from 33 broadband seismometers in Taiwan within a temporal span of approximately one year (from June 2015 to June 2016) are utilized in this study. The common-mode ground vibrations in most seismic stations are composed by cumulating the first twenty principal components. The common-mode ground vibrations are sliced into several time spans using a 5-day moving window with one-day steps to show time-varying changes. The common-mode data in each time span are transferred into the frequency domain using the Fourier transform. We next superimpose the amplitude based on the occurrence time of the 20 M >= 4 earthquakes during the one-year temporal span. The superimposed amplitudes are normalized using the frequency-dependent average values computed from the superimposed amplitude 30 days before and after earthquakes via the temporal division. Fig. 3 shows the amplitude ratios associated with the M>= 4 earthquakes. Distinct patterns in the amplitude-frequency distributions can be observed before and after earthquakes. The frequency is close to 5×10^{-4} Hz approximately 40 days before the quakes and tends to be high near 10^{-3} Hz a few days before the quakes. The amplitudes of the variable frequency patterns are proportional to the earthquake magnitude (Fig. S5).

https://doi.org/10.5194/nhess-2020-47
Preprint. Discussion started: 24 February 2020

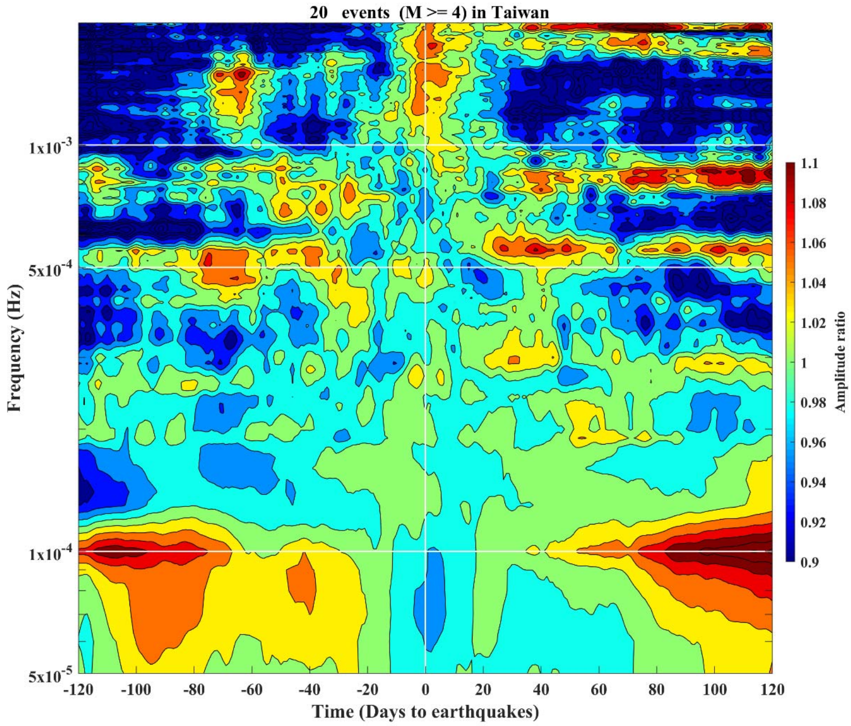

Fig. 3. The amplitude ratios of the superimposed time-frequency-amplitude distribution associated with the 20 M >= 4 earthquakes in Taiwan.

Walczak et al. (2017) repeatedly observed stressed rocks exciting long-period vibrations during rock mechanics experiments. Leissa (1969) reported that the resonance frequency of an object is proportional to its Young's modulus and exhibits an inverse relationship to its mass. Accordingly, we assume that the earthquake-related stress accumulates in the volume of a square sheet with a width of 100 km based on a distance of 50 km away from a quake due to the significant increase in the seismic density (Figs. 1 and 2). The thickness of the volume is directly ranged between 500 meters and 1000 meters. The stressed volume is placed horizontally at the depth of the hypocenter that excites vibrations at the resonance frequency before rupture. Note that we do not take the fault type and shape of the stressed object into consideration.

The resonance frequency near 3×10^{-4} Hz can be derived from the square sheet (Fig. 4).

Previous studies (Cappa, 2009; Bilham R. et al., 2017) reported that the Young's modulus is strengthen a few days before earthquakes. However, enhancement of the Young's modulus is not a major factor driving the high resonance frequency at 10^{-3} Hz. When the width of the sheet is determined to be the hot fault region as 40 km with a significant increase of seismic density a few days before the quakes, a resonance frequency near 10^{-3} Hz (Fig. 3) can be reproduced by the same model (Leissa, 1969). The results suggest that the resonance frequency is variable from ~3×10^{-4} Hz to ~10^{-3} Hz between 40 days and a few days along with the forthcoming earthquakes. In agreement with the spatiotemporal domain of the relatively-small quakes from the earthquake catalogs, the superimposition results of continuous seismic waveforms and the resonance frequency models suggest that the phenomenon of variable frequency may exist tens of days before earthquake occurrence and can be retrieved by broadband seismometers.

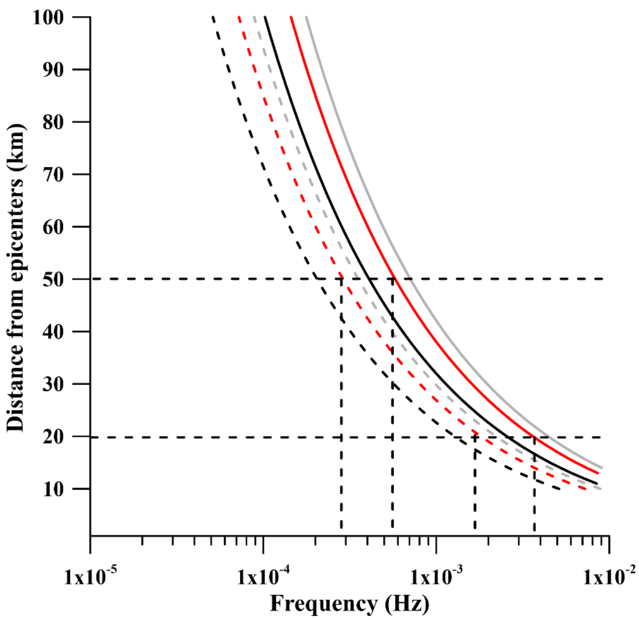

Fig. 4. Relationships between the width and resonance frequency of a square sheet.

https://doi.org/10.5194/nhess-2020-47
Preprint. Discussion started: 24 February 2020

Natural Hazards and Earth System Sciences
Open Access
Discussions

We assume that the resonant area is a square sheet with all sides simply supported. According to Leissa (1969), the resonance frequency of such a square sheet can be estimated using the formula $f=\frac{1}{2\pi}\sqrt{\frac{Eh^2}{12(1-\upsilon^2)\rho}}[(\frac{m\pi}{a})^2+(\frac{n\pi}{b})^2]$, where E is Young's modulus; h is the thickness of the sheet; ρ is the mass density; υ is the Poisson's ration; a and b are the lengths of the plate; and m and n are integers. In this study, a equals b as the sheet is square and these values are assumed to be two times the distance from the epicenter. The solid and dashed curves indicate the relationships between the width and resonance frequencies, as computed at thicknesses of 1000 m and 500 m, respectively. The black, red and grey colors are computed by using the Young's modulus of 50 GPa, 100 GPa and 150 GPa respectively. Notably, m and n are taken to be 1 to estimate the relationship based on a fundamental mode. Average density of the crust is 2700 kg/m^3 (Vilarrasa and Carrera, 2015). Poisson's ratio is 0.3.

5. Conclusion

In short, the process of stress migration in the spatiotemporal domain can be concluded from tracing the increase of seismicity according to the 10-year earthquake catalogs from dense seismic arrays in Taiwan and Japan. Areas with the increase of seismicity where stress accumulates in the crust triggering earthquakes are serious underestimation using a sparse seismic array. Seismicity initially increases around hypocenters, and this can be observed more than 50 days before quakes through superimposing large numbers of earthquakes. The seismicity gradually increases along with the expansion of areas from fault zones to an area widely covering an epicentral distance close to 50 km approximately 20–40 days before earthquakes. The crustal resonance exists at a frequency near 3×10^{-4} Hz when the expansion becomes insignificant. Instead of the spatial expansion, the sharp increase of seismicity around the hot regions suggests stress accumulation in fault zones generating crustal resonance at a frequency of up to $\sim10^{-3}$ Hz in the few days before earthquakes. Most broadband seismometers can observe the variable frequency of ground vibrations in Taiwan due to

https://doi.org/10.5194/nhess-2020-47
Preprint. Discussion started: 24 February 2020

the comprehensive spatial coverage of resonant signals. The variable frequency depends on various stress-dominant areas that can be supported by the potential crustal resonance model. Seismic arrays comprise dense seismometers with a wide coverage are beneficial for monitoring the comprehensive process of stress migration in the spatiotemporal domain leading up to a faraway and forthcoming mainshock.

Acknowledgements. The authors appreciate scientists who devote to maintain instruments in the field and data centers in the office that leads chances to expose such interesting geophysical phenomena and understand potential processes during seismogenic periods. This work is supported by National Natural Science Foundation of China (Grants No. 41474038 and 41774048), the Spark Program of Earthquake Science of China (Grant No. xh17045), Ministry of Science and Technology of Taiwan (Grants No. MOST 106-2116-M-194-016- and MOST 106-2628-M-008-002), and Sichuan earthquake Agency-Research Team of GNSS based geodetic tectonophysics and mantle-crust dynamics of Chuan-Dian region (Grant No. 201804).

References

Adams, J.B., Mann, M.E., and Ammann, C.M.: Proxy evidence for an El Niño-like response to volcanic forcing, Nature, 426, 274–278, 2003.

Bilham R., Mencin, D., Bendick, R., and Bürgmann, R.: Implications for elastic energy storage in the Himalaya from the Gorkha 2015 earthquake and other incomplete ruptures of the Main Himalayan Thrust, Quatern. Int., 462, 3–21, 2017.

Cappa, F.: Modelling fluid transfer and slip in a fault zone when integrating heterogeneous hydromechanical characteristics in its internal structure, Geophys. J. Int., 178, 1357–1362, 2009.

Chang, C.H.: Introduction to the Meteorological Bureau Earthquake Monitoring Network, Taiwan Earthquake Research Center Newsletter, 2014.

Chree, C.: Some phenomena of sunspots and of terrestrial magnetism at Kew observatory, Phil. Trans. R. Soc., 212, 75, 1913.

https://doi.org/10.5194/nhess-2020-47
Preprint. Discussion started: 24 February 2020

Ellsworth, W.L., and Beroza, G.C.: Seismic evidence for an earthquake nucleation phase, Science, 268, 851–855, 1995.

Gardner, J. K., and Knopoff, L.: Is the sequence of earthquakes in southern California, with aftershocks removed, Poissonian? Bull. Seism. Soc. Amer. 64, 1363–1367, 1974.

Hocke, K., Oscillations of global mean TEC, J. Geophys. Res., 113, A04302, https://doi.org/10.1029/2007JA012798, 2008.

Jolliffe, I.T.: Principal Component Analysis, second edition, Springer, 2002.

Kato, A., and Obara, K.: Step-like migration of early aftershocks following the 2007 Mw 6.7 Noto-Hanto earthquake, Japan, Geophys. Res. Lett., 41, 3864–3689, https://doi.org/10.1002/2014GL060427, 2014.

Kato, A., Obara, K., Igarashi, T., Tsuruoka, H., Nakagawa, S., and Hirata, N.: Propagation of slow slip leading up to the 2011 Mw9.0 Tohoku-Oki earthquake, Science, 335, 705–708, https://doi.org/10.1126/science.1215141， 2012.

Kawamura, M., Chen, C.C., and Wu, Y.M.: Seismicity change revealed by ETAS, PI, Z-value methods: A case study of the 2013 Nantou, Taiwan earthquake, Tectonophysics, 634, 139–155， 2014.

Leissa, A.W., Vibrations of plates. Ohio State University, Columbus, Ohio, 1969.

Liu, S., Tang, C.C., Chen, C.H., and Xn, R.: Spatiotemporal Evolution of the 2018 Mw 6.4 Hualien Earthquake Sequence in Eastern Taiwan, Seismol. Res. Lett., https://doi.org/10.1785/0220180389， 2019.

Reasenberg, P.： Second-order moment of central California seismicity, 1969-82, J. Geophys. Res., 90, 5479–5495, 1985.

Reasenberg, Paul A.: Foreshock occurrence before large earthquakes, J. Geophys. Res., 104, 4755–4768, 1999.

Scholz, C.H.： The Mechanics of Earthquakes and Faulting. second edition, Cambridge University Press, Cambridge, UK, 2002.

Uhrhammer, R.: Characteristics of northern and southern California seismicity:

Earthquake Notes, 57, 21, 1986.

Vidale, J., Mori, J.， and Houston, H.: Something wicked this way comes: Clues from foreshocks and earthquake nucleation, Eos Trans. AGU, 82, 68, 2001.

Vilarrasa, V., and Carrera, J.: Geologic carbon storage is unlikely to trigger large earthquakes and reactivate faults through which CO_2 could leak, P. Nat. Acad. Sci. USA, 112(19), 5938–5943, https://doi.org/10.1073/pnas.1413284112, 2015.

Walczak, P. et al.: Real time observation of granular rock analogue material deformation and failure using nonlinear laser interferometry, arXiv preprint, arXiv:1705.03377v1, 2017.

Wen, Y.-Y., and Chen, C.-C. Chen: Seismicity variations prior to the 2016 ML 6.6 Meinong, Taiwan earthquake, Terr. Atmos. Ocean. Sci., 28, 739–744, https://doi.org/10.3319/ TAO.2016.12.05.01, 2017.

Wiemer, S.: A Software Package to Analyze Seismicity: ZMAP, Seismol. Res. Lett., 72, 373–382, https://doi.org/10.1785/gssrl.72.3.373, 2001.

Wiemer, S.：A software package to analyze seismicity: ZMAP”, Seism. Res. Lett., 72, 373–382, 2001.

Data available

The earthquake catalogs of Taiwan and Japan were obtained from the Central Weather Bureau (https://www.cwb.gov.tw/), and the Japan Meteorological Agency (JMA; https://www.jma.go.jp/jma/indexe.html), respectively. Seismic waveform data in Taiwan were provided by the Seismic Array of NCREE in Taiwan (SANTA; https://www.ncree.narl.org.tw/; please find the bottom for the English version in the top right side). The downsampled seismic waveforms with the temporal interval of 10 seconds can be utilized to reproduce the analytical results in this study through the MATLAB software that can be download at https://doi.org/10.5061/dryad.1jwstqjqq.

https://doi.org/10.5194/nhess-2020-47
Preprint. Discussion started: 24 February 2020

Natural Hazards and Earth System Sciences
Open Access
Discussions

Author contribution

Y.Y.S. contributed discussion and revision; S.W. contributed discussion and revision; P.H. contributed data collection; L.C.L. contributed discussion and revision; H.Z.Y. contributed discussion; X.Z. contributed discussion; Y.G. contributed discussion; C.C.T. contributed discussion and revision; C.H.L. contributed discussion and revision; J.Y.L. contributed discussion and revision.

Competing interests

The authors declare that they have no known competing financial interests or personal relationships that could have appeared to influence the work reported in this paper.